Synthetic Structural Imaging (SSI):

A New Ultrasound Method for Tracking Breast Cancer Morphology

Alan A. Winder, Bahram Jadidian
J&W Medical LLC
Westport CT USA

Robert Muratore
Quantum Now LLC
Huntington NY USA
wave@quantumnow.com

Abstract—A new signal interrogation concept, based on Synthetic Structural Imaging (SSI) physics, has been developed to guide therapies. The SSI method was previously successful in radar and sonar imaging; here it is demonstrated for acoustic scattering from penetrable biological targets. Operating at ultrasonic frequencies of several hundred kilohertz, SSI trades the higher resolution of typical B-mode ultrasound imaging for a significantly stronger correlation to target shape and volume, which are among the primary tissue classifiers. Tissue phantom models were fabricated with embedded spheroidal inclusions ranging from 2.41 mm through 6.3 mm in diameter. The phantom medium was 10 wt% porcine gelatin and the inclusions were 28 wt% porcine gelatin. The inclusion dimensions were measured with calipers. The phantom was interrogated with two impulse-excited Panametrics transducers: a model V301 with a peak frequency of 0.50 MHz and a -6 dB bandwidth of 81%, and a model V314 with a peak frequency of 0.99 MHz and a -6 dB bandwidth of 77%. The backscattered RF data were digitized, recorded, and digitally bandpass-filtered. The experimental profile functions were computed. Volumes were estimated by integrating the experimental profile functions. SSI-determined volume ratios were demonstrated to be within 7% to 18% of caliper-determined volume ratios.

Keywords-Synthetic Structural Imaging; SSI; ultrasound, monitoring; morphology; breast; prostate; cancer; tumor; volume; oncology; organ; fetus; fetal development; 3D; three dimensional imaging; neoadjuvant therapy

I. INTRODUCTION

There is a clinical need for three dimensional imaging. Generally, a caregiver or a scientist wants to track changes in the size, shape, and composition of regions of interest (ROIs) in the body. For example, neoadjuvant chemotherapy is used to shrink breast cancer tumors preceding lumpectomies [1,2]; oncologists monitor tumor size and metastatic spread to determine the optimal time for surgery. Preoperative breast imaging technologies [3-5] are employed to provide sufficient tissue definition to remove the cancerous tissue, leaving clear margins that can support a positive breast conservation approach. Obstetricians study fetal development; total fetal volume and development of specific organs are monitored in at-risk pregnancies. Ideally, volumetric studies should be quick and simple to apply, for bedside application, for ad lib monitoring, for patient comfort and compliance, and for use in economically disadvantaged clinics. Ultrasonic synthetic structural imaging (SSI), adapted from radar airwing identification studies [6] and previously applied to sonar imaging [7], has the potential to become an ideal volumetric imaging tool for the above medical applications. This paper presents the results of SSI volumetric studies in biological phantoms to simulate the tracking of breast cancer morphology.

This work was supported in part by the United States Department of Defense Breast Cancer Research Program Concept Award BC076704.

II. BACKGROUND

SSI physics [8,9] is a low frequency technique that builds on the concept of the ramp response, derived from the upper Rayleigh and low resonance regions of the target backscattered response. Similar to conventional high frequency imaging, the SSI method is direction-dependent, but is considerably more robust. It has less resolution then conventional techniques but its correlation to shape is much stronger. The ramp response signature is the basis for low frequency characterization, where the derived physical optics approximation of the target's ramp response $R(t)$ is directly proportional to the target cross-sectional area $A(r)$ along the direction of propagation of the incident field, and is expressed as

$$R(t) = \left(-\frac{1}{\pi c^2} \right) A(r), \tag{1}$$

where t is time, c is the velocity of propagation in the medium, and $r = ct/2$ is the radial distance. Thus, the ramp response is a unique low frequency measure of target shape and orientation. If the ramp response is integrated over the insonified target in the direction of the propagating wave, the resulting parameter is a *spatially-invariant measure* of the target volume (V):

$$V = \int_{r_1}^{r_2} A(r)dr \approx \int R(t)dt. \tag{2}$$

This "one-look" interrogation property is unique to the SSI method and results in minimal data acquisition time, producing minimum target movement and less exposure time. Furthermore, the ripples in the ramp response provide unique information concerning the target's structural parameters and composition that will enhance the classification process.

Low frequency imaging is characterized by a narrow bandwidth and a low absorption loss while high frequency imaging is characterized by a wide bandwidth and a high absorption loss. The latter will tend to shorter tissue depths for characterization. The high frequencies characterize the fine detail of the target while, as stated above, the lower frequencies provide information as to overall dimension and

978-1-4244-7946-7/10/$26.00 ©2010 IEEE

approximate shape. Higher frequencies can obviously sharpen the image and remove spatial ambiguities but without low frequency information there is no image.

The proposed hypothesis of the study is that the SSI method, shown to be valid for steel-hulled structures, is also valid for acoustic, elastic scattering from penetrable biological tissue targets, such as breast tissue, and can be used as a pre-surgical planning tool in neoadjuvant chemo-therapy treatment.

III. METHODS

Gelatin phantoms were constructed, and caliper measurements of inclusions were compared to SSI estimates. The procedure is illustrated in Figure 1.

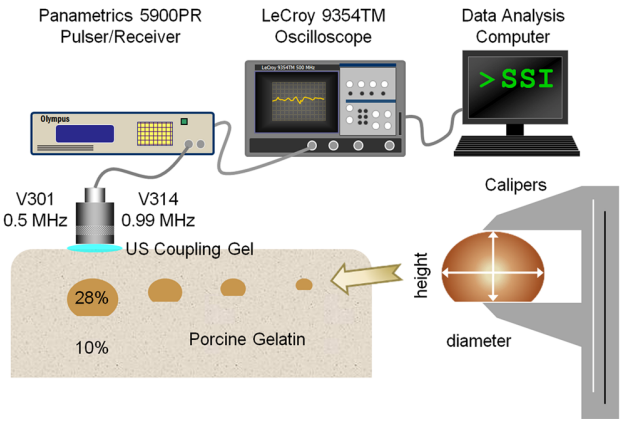

Figure 1. Caliper measurements of porcine gel inclusions in a phantom were compared to SSI analysis of backscattered RF ultrasound signals.

A. Phantoms

Phantoms were fashioned from porcine skin gelatin (Type A, approximately 175 bloom, Sigma Chemical Co., St. Louis MO USA); 10% by weight gelatin was used for the phantom matrices, and 28% by weight gelatin was used for inclusions. Appropriate amounts of gelatin powder were dispersed and then dissolved in water at room temperature and 65°C, respectively. The solutions were subsequently filtered through cheesecloth, degassed under -51 kPa pressure, and cooled down to room temperature. Inclusions with various diameters were formed by setting droplets of a partially gelled 28% solution on the tips of plastic syringes. The inclusions had an oblate spheroid shape with a flattened bottom. Before being embedded in the matrices, the inclusion heights and diameters were measured with calipers. In each phantom, the vertices of the inclusions were aligned at equal depth from the surface of the matrix, with flat sides distal to the surface as shown in Figure 1. The depth of the inclusions was different in different matrixes, ranging from 20 mm to 30 mm.

B. Acoustic System

Ultrasound signals were obtained from f/1.5 single-element immersion transducers (Panametrics NDT, Waltham MA USA). Two models were used in separate experiments. According to the manufacturer's calibration certificates, model V301 has a diameter of 25 mm and a focal length of 37.0 mm, and its power spectrum exhibits a peak frequency of 0.50 MHz and a -6 dB bandwidth of 81%; model V314 has a diameter of 18 mm and a focal length of 26.2 mm, and its power spectrum exhibits a peak frequency of 0.99 MHz and a -6dB bandwidth of 77%. The transducers were coupled to the gelatin phantoms with commercial ultrasound coupling gel. A pulser-receiver (model 5900PR, Panametrics NDT) was used to excite the transducers with an impulse and to receive the backscattered A-mode signals. With the 0.50 MHz transducer, 25 µJ pulses were used and 64 sweeps were averaged; with the 0.99 MHz transducer, 100 µJ pulses were used and 512 sweeps were averaged. The received signals were acquired with a digitizing storage oscilloscope (model 9354TM, LeCroy Corp., Chestnut Ridge NY USA) at sample rates of 10 MS/s and 20 MS/s. Data from bulk porcine gelatin (50 mm diameter, 100 mm thick) was used to determine speed of sound. The pulse-echo method was employed to measure the longitudinal acoustic velocities of the 10wt% and 28wt% gels.

C. SSI Analysis

Data from the phantoms were analyzed with the SSI routine using the MATLAB programming environment (release 2700b, The MathWorks, Inc., Natick MA USA) running under the Windows XP operating system (Microsoft Corp., Redmond WA USA). RF signals were sorted and bandpass-filtered. Experimental profile functions (EPFs) [10] were computed and integrated. Relative volume estimates of the dense phantom inclusions were represented as ratios of integrated EPF values.

IV. RESULTS

In the 10% porcine gelatin, the speed of sound was estimated to be 1530 m/s; in the 28% porcine gelatin, the speed of sound was estimated to be 1684 m/s. Thus, in the gelatin matrix, the predominate wavelengths of the ultrasound beams from the V301 and V314 transducers were 3.06 mm and 1.55 mm respective, and the -6 dB beam widths in the focal region were estimated as wavelength·f-number to be 4.6 mm and 2.2 mm respectively.

An example of a set of backscattered data from the V314 transducer is shown in Figure 2. In this trial, the inclusions (2.5 mm diameter x 2.35 mm height, and 6.3 mm diameter x 4.40 mm height) were at a depth of 30 mm in the phantom, and 512 sweeps were averaged. The experimental profile functions obtained from these data sets are shown in Figure 3, normalized to the peak of the larger EPF. Figure 4 summarizes the estimated volume ratios. Acoustic estimates originating with the V301 transducer are shown as gray squares; estimates originating with the V314 transducer are shown as black diamonds. Ideally, the volume ratios estimated by the acoustic SSI technique would match the volume ratios obtained by the caliper measurements. Discrepancies ranged from 7% to 18%.

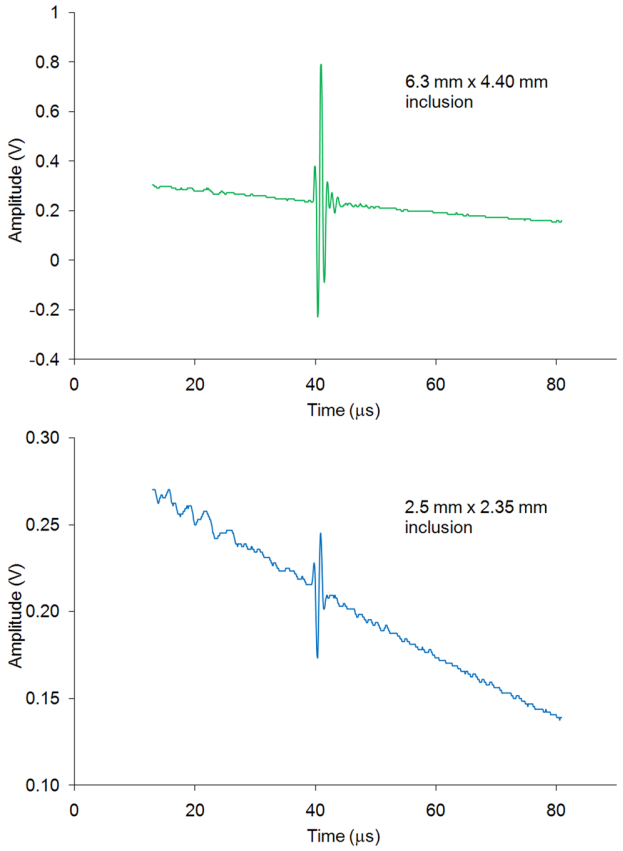

Figure 2. Average over 512 sweeps of backscattered A-mode data obtained with a Panametrics V314 transducer for two inclusions at a depth of 30 mm in the gelatin phantom.

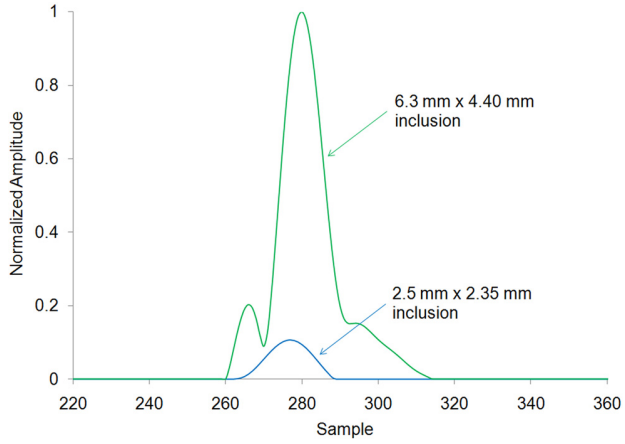

Figure 3. Experimental profile functions derived from the backscattered echoes shown in Figure 2.

V. Discussion

Operating at ultrasonic frequencies of several hundred kilohertz, SSI trades the higher resolution of typical B-mode ultrasound imaging for a significantly stronger correlation to target shape and volume, which are among the primary tissue classifiers. The potential benefits of the SSI method, operating with noninvasive low frequency ultrasound, are considerable. Perhaps the most important application is the therapeutic monitoring of tumor shrinkage with chemo-radiation therapy or high intensity therapeutic ultrasonic ablation, providing estimates of the size of dense masses in breast and other tissues. The SSI method will also facilitate biopsies of tumors detected with MRI which are not readily detectable on a mammogram, i.e., those with diameters less than 5 mm.

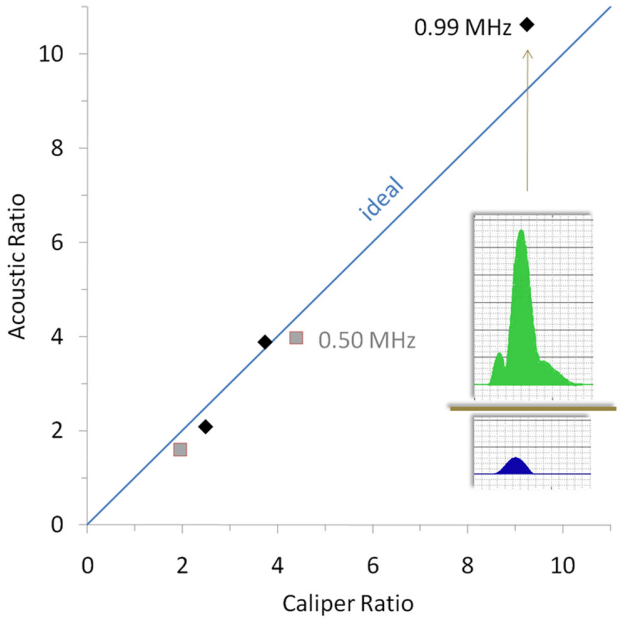

Figure 4. The ratios of the volume estimates obtained by the acoustic SSI method are compared to the ratios of volume estimates obtained from caliper measurements of dense gelatin inclusions in the phantom. Acoustic data obtained from the Panametrics V301 transducer are shown as gray squares; data from the V314 transducer are shown as black diamonds. The inset illustrates the ratio of the integrals of the EPFs presented in Figure 3, approximately 10.6.

VI. Conclusions

SSI effectively estimates biological phantom volumes. Accurate volume estimate requires appropriate matching of transducer excitation and the product of the wavenumber (k) and maximum scatterer size (L), (kL). Therefore, within the acoustic and signal processing constraints of the tests, the SSI method has been shown to be valid for acoustic, elastic scattering from penetrable biological tissue targets.

References

[1] S. J. Vinnicombe, A. D. MacVicar, et al., "Primary breast cancer: mammographic changes after neoadjuvant chemotherapy, with pathologic correlation," Radiology, vol. 198, pp. 333-340, Feb. 1996.

[2] V. Londero, M. Bazzocchi, et al., "Locally advanced breast cancer: comparison of mammography, sonography and MR imaging in evaluation of residual disease in women receiving neoadjuvant chemotherapy," Eur. Radiology, vol. 14, pp. 1371-1379, Aug. 2004.

[3] E. A. Morris, "Diagnostic breast MR imaging: current status and future directions," Magn. Reson. Imaging Clin. N. Am., vol. 18, pp. 57-74, Feb. 2010.

[4] E. Thornton, S. Looby, and L. Hanlon, “Preoperative breast imaging guides surgical management,” Diagnostic Imaging Asia Pacific, pp. 34-41, Aug. 26, 2008.

[5] S. H. Park, B. I. Choi, et al., “Volumetric tumor measurement using three-dimensional ultrasound: in vitro phantom study on measurement accuracy under various scanning conditions, Ultrasound Med. Biol., vol. 30, pp. 27-34, Jan. 2004.

[6] A. A. Ksienski, Y. Lin, and L. J. White, “Low-frequency approach to target identification,” Proc. IEEE, vol. 63, pp. 1651-1660, Dec. 1975.

[7] A. A. Winder, (U) Synthetic target imaging classification (C), Contract No. MDA 903-81-C-0321, DARPA Order No. 3755, Technical Report No. 186, Oct. 30, 1992.

[8] E. M. Kennaugh and D. L. Moffatt, “Transient and impulse response approximation,” Proc. IEEE, vol. 53, pp. 893-901, Aug. 1965.

[9] J. D. Young, “Radar imaging from ramp response signatures,” IEEE Trans. Antenna Propagat., vol. AP-24, pp. 276-282, Mar. 1976.

[10] H. Lin and A. A. Ksienski, “Optimum frequencies for aircraft classification,” IEEE Trans. Aerospace Elect. Syst., vol. AES-17, pp. 656-665, Sept. 1981.